Nucleotide-Induced Conformational Changes in P-glycoprotein and in Nucleotide Binding Site Mutants Monitored by Trypsin Sensitivity†

Michel Julien and Philippe Gros*

Department of Biochemistry, McGill University, Montréal, Québec, Canada, H3G 1Y6

Received November 30, 1999; Revised Manuscript Received February 1, 2000

ABSTRACT: Limited trypsin digestion was used to monitor nucleotide-induced conformational changes in wild-type P-glycoprotein (Pgp) as well as in nucleotide binding domain (NBD) Pgp mutants. Purified and reconstituted wild-type or mutant mouse Mdr3 Pgps were preincubated with different hydrolyzable or nonhydrolyzable nucleotides, followed by limited proteolytic cleavage at different trypsin:protein ratios. The Pgp tryptic digestion products were separated by SDS−PAGE followed by immunodetection with the mouse monoclonal anti-Pgp antibody C219, which recognizes a conserved epitope (VVQE/AALD) in each half of the protein. Different trypsin digestion patterns were observed for wild-type Pgp incubated with $MgCl_2$ alone, MgADP, MgAMP·PNP, MgATP, and MgATP + vanadate. A unique trypsin digestion profile suggestive of enhanced resistance to trypsin was observed under conditions of vanadate-induced trapping of nucleotides (MgATP + vanadate). The trypsin sensitivity profiles of Pgp mutants bearing either single or double mutations in Walker A (K429R, K1072R) and Walker B (D551N, D1196N) sequence signatures of NBD1 and NBD2 were analyzed under conditions of vanadate-induced trapping of nucleotides. The proteolytic cleavage pattern observed for the double mutants K429R/K1072R and D551N/D1196N, and for the single mutants K429R, K1072R, and D1196N were similar and clearly distinct from wild-type Pgp under the same conditions. This is consistent with the absence of ATP hydrolysis and of vanadate-induced trapping of 8-azido-ADP previously reported for these mutants [Urbatsch et al. (1998) *Biochemistry 37*, 4592−4602]. Interestingly, the trypsin digestion profiles observed under vanadate-induced trapping for the D551N and D1196N mutants were quite different, with the D551N mutant showing a profile resembling that seen for wild-type Pgp. The different sensitivity profiles of Pgp mutants bearing mutations at the homologous residue in NBD1 (D551N) and NBD2 (D1196N) suggest possible structural and functional differences between the two sites.

Overexpression of P-glycoprotein (Pgp)[1] is associated with multidrug resistance in vitro and in vivo (*1*). Pgp is a plasma membrane protein that acts as a drug transporter to reduce intracellular drug accumulation by an ATP-dependent mechanism (*2*, *3*). Pgp is composed of two symmetric and homologous halves, each encoding six transmembrane (TM) domains and one nucleotide binding domain (NBD) (*1*). This structural unit (6TM, 1NBD) defines the ABC (ATP-binding cassette) family of membrane transporters, which has members in bacteria, yeast, parasites, nematodes, plants, and mammals (*4*). In mammals, this family includes transporters for peptides (*5*), chloride ions (*6*), acylated fatty acids (*7*, *8*), bile acids (*9*), and other substrates (*10*).

A large body of published data indicates that drug binding to Pgp occurs through interactions with the TM domains, while ATP hydrolysis to energize transport is mediated by the NBDs (reviewed in ref *1*). Pgp has a basal ATPase activity (*2*, *11*) that can be strongly stimulated by several Pgp substrates or inhibitors of transport (*3*). Both predicted NBDs of Pgp contain Walker A and Walker B sequence signatures characteristic of several ATP-binding proteins or ATPases (*12*), and independent mutations of these sequences in NBD1 or NBD2 (Walker A, K429, K1072; Walker B, D551, D1196) completely abolish Pgp-mediated drug resistance and drug transport (*13*−*16*). Such Walker A and B mutants can bind MgATP but can no longer hydrolyze MgATP, as measured in ATPase assays or by vanadate-induced trapping of 8-azido-ADP (*15*−*17*). Based on these and other studies, an alternate site catalysis model has been proposed for ATP hydrolysis by Pgp, with complete cooperativity between the two NBDs (reviewed in ref *18*). In this model, both NBDs are functionally equivalent and can each hydrolyze ATP.

The mechanism by which ATP hydrolysis at one or both NBDs energizes drug translocation across the membrane remains a poorly understood aspect of Pgp. Several experi-

† This work was supported by research grants to P.G. from the Medical Research Council of Canada (MRC). P.G. is an International Research Scholar of the Howard Hughes Medical Institute and is supported by a Senior Scientist Award of the MRC.

* To whom correspondence should be addressed at the Department of Biochemistry, McGill University, 3655 Drummond St., Room 907, Montréal, Québec, Canada, H3G 1Y6. Phone: 514-398-7291. Fax: 514-398-2603. E-mail: gros@med.mcgill.ca.

[1] Abbreviations: ABC, ATP-binding cassette; ADP, adenosine diphosphate; AMP, adenosine monophosphate; AMP·PNP, adenylyl-imido diphosphate; ATP, adenosine triphosphate; CFTR, cystic fibrosis transmembrane conductance regulator; DM, *n*-dodecyl-*β*-D-maltoside; DTT, dithiothreitol; MIANS, 2-(4-maleimidoanilino)naphthalene-6-sulfonic acid; NBD, nucleotide binding domain; Pgp, P-glycoprotein; PMSF, phenylmethylsulfonyl fluoride; SDS−PAGE, sodium dodecyl sulfate−polyacrylamide gel electrophoresis; TM, transmembrane.

10.1021/bi992744z CCC: $19.00
Published on Web 03/23/2000

mental approaches have been used to monitor possible conformational changes in Pgp associated with drug binding, ATP binding, and/or hydrolysis by the protein. Mechetner et al. (*19*) studied differential immunoreactivity of the mouse monoclonal anti-Pgp antibody UIC2, that recognizes an extracellular epitope of Pgp. They have used this antibody to identify possible conformational transition states in Pgp associated with drug binding, ATP binding, or hydrolysis. Indeed, they noted that UIC2 immunoreactivity was increased by Pgp substrates, by ATP depleting agents, and by mutational inactivation of both NBDs. On the other hand, tryptophan fluorescence has been used to monitor changes in local environment and to obtain dynamic structural information in various membrane proteins including F1-ATPase (*20, 21*), ArsA (*22, 23*), and the lactose permease (*24*). Acrylamide and potassium iodide quenching of Pgp endogenous tryptophan fluorescence was used to monitor structural changes associated with interactions with nucleotides and drug substrates (*25, 26*). Important structural changes were noted after binding of MgATP (but not MgADP) and following interactions with anthracycline derivatives that are transported or not by Pgp (*26*). Pgp labeled by a fluorescent probe, 2-(4-maleimidoanilino)-naphthalene-6-sulfonic acid (MIANS), at two cysteine residues in the NBDs was used to monitor interaction with nucleotides (*27, 28*), and also to estimate distances of the NBDs with the lipid bilayer in a reconstituted system (*29*). Together, these studies have shown that Pgp undergoes important conformational changes after interaction with nucleotides or drug substrates.

Protease sensitivity has also been used extensively to monitor structural changes in proteins associated with interactions with ligand, or with other protein, or to monitor the effect of point mutations on overall protein structure. It has been used both for soluble proteins, such as replication protein A (*30*), but also for integral membrane proteins including phospholipid scramblase (*31*), bacterial Na^+/H^+ antiporter (*32*), and yeast plasma membrane PMA2 H^+-ATPase (*33*), and recently to probe the blockage of conformational maturation of the ΔF508 mutant variant of CFTR (*34*). In the case of Pgp, nucleotide- and drug-induced conformational changes have been studied by trypsin sensitivity using isolated inside-out membrane vesicles and immunoblotting with a mouse monoclonal anti-Pgp antibody MD7 directed against the segment linking TM8 and TM9 in the C-terminal half of the protein (*35, 36*). Different conformations were detected with this antibody, including one with MgATP/MgADP and another with $MgCl_2$ alone. Drug binding to Pgp was also found to cause a conformational change, but that was different than that caused by nucleotides. In addition, incubation of Pgp with both drugs and nucleotides produced a conformation that was distinct from the conformation stabilized by either ligand alone (*35*).

In the present study, we used highly purified preparations of Pgp reconstituted in lipids to monitor the effect of various hydrolyzable and nonhydrolyzable nucleotides on conformational changes in the protein. We have used partial trypsin digestion at different trypsin-to-protein ratios to monitor possible conformational changes in Pgp. Several conformations were detected by this approach, including a unique protease-resistant conformation observed under conditions of vanadate-induced trapping of nucleotide (MgATP + vanadate). The presence or absence of this conformation was then monitored in various catalytically inactive Pgp mutants bearing mutations in key residues of the Walker A (K429R, K1072R) and Walker B motifs (D551N, D1196N) of either or both nucleotide binding sites (NBD1, NBD2) of the protein. The MgATP + vanadate conformation was abrogated by mutation of both NBDs (NBD1/NBD2) and by single mutations at either D1196N, K429R, or K1072R, consistent with the loss of ATPase activity in these mutants. Surprisingly, we observed that MgATP + vanadate can still induce a conformation similar to wild-type in the single mutant D551N, despite its apparent lack of ATPase activity.

EXPERIMENTAL PROCEDURES

Expression, Purification, and Reconstitution of P-glycoprotein. The wild-type mouse Mdr3 Pgp and also Pgp mutants bearing either single or double mutations in the Walker A (K429R, K1072R) and Walker B (D551N, D1196N) sequence signatures of NBD1 and NBD2 were constructed into pHIL-D2 plasmid vector (Invitrogen) and overexpressed in the yeast *Pichia pastoris* as previously described (*15*). The conditions for expression, solubilization, and purification of the wild-type and mutant Pgp from 2 L cultures induced with methanol were exactly as we have previously described (*15*). Briefly, total microsomal membranes were isolated by centrifugation on a discontinuous sucrose density gradient. Fifty milligrams of the membrane fraction banding at the 16/31% sucrose interface was precipitated with 10 mM $MgCl_2$ (30 min at 4 °C) to remove EGTA and DTT, and recovered by centrifugation (16000*g*, 20 min at 4 °C). Membrane pellets were resuspended in buffer containing 50 mM Tris, pH 8, 20% glycerol, 50 mM NaCl, 5 mM imidazole, 0.5 mM β-mercaptoethanol (buffer A) and solubilized by adding an equal volume of 0.6% L-α-lysophosphatidylcholine (lyso-PC, from egg yolk, 99% pure, Sigma) in buffer A at a final protein concentration of 2 mg/mL, followed by gently vortexing at 20 °C. Samples were cleared of particulate material by centrifugation (60000*g*, 30 min at 4 °C), and solubilized proteins were mixed with 700 μL of packed Ni−NTA resin (Qiagen), equilibrated with buffer A, followed by incubation at 4 °C for 20 h with continuous rotation. The resin was transferred to a column and washed extensively with 20 bed volumes of 50 mM Tris, pH 8, 20% glycerol, 50 mM NaCl, 5 mM imidazole, 0.5 mM β-mercaptoethanol, 0.1% *n*-dodecyl-β-D-maltoside (DM) (buffer B) followed by an additional 20 bed volumes of buffer B containing 20 mM imidazole. Proteins bound to the Ni−NTA resin were eluted with 3 mL of a buffer containing 50 mM Tris-HCl, pH 8.0, 20% glycerol, 80 mM imidazole, and 0.1% DM. All buffers used in the purification procedures contained freshly prepared protease inhibitors (1 mM PMSF, 10 μg/mL leupeptin, 10 μg/mL pepstatin A; Boehringer). For reconstitution, the purified protein was incubated with 0.25% *Escherichia coli* lipids (acetone/ether preparation) and 5 mM DTT for 30 min on ice, followed by dialysis (16 h, 4 °C) against a buffer containing 50 mM Tris-HCl, pH 7.4, 0.1 mM EGTA, and 1 mM DTT. The reconstituted protein was concentrated by centrifugation (200000*g*, 2 h, 4 °C), and was resuspended at a final concentration of 0.7 μg/μL in dialysis buffer. This final suspension was aliquoted and stored at −80 °C until use.

Trypsin Treatment of Pgp. Reconstituted wild-type and mutant Pgp variants (3.5 μg in 5 μL) were preincubated with different nucleotides (final volume 10 μL), as indicated in the text, for 15 min at 37 °C. The final concentration of the nucleotides was 10 mM except for vanadate (200 μM final concentration). Trypsin (2 μL), from different stock solutions prepared in 10 mM HCl (20, 10, 5, 2, 1, 0.5, 0.25 mg/mL, and 125, 62.5, 31.25, 15.6, 7.8, and 3.9 μg/mL), was added to the Pgp nucleotide mixtures to obtain the desired trypsin:Pgp ratios (w:w), followed by incubation for 15 min at 37 °C. The reaction was stopped by addition of 10 μL of Laemmli sample buffer [5% (w/v) SDS, 25% (v/v) glycerol, 0.125 M Tris-HCl, pH 6.8, 40 mM DTT, 0.01% pyronin Y] followed by further incubation for 30 min at 37 °C. The peptide fragments were separated by SDS−PAGE on 12% polyacrylamide gels, followed by transfer onto nitrocellulose membranes. For immunodetection of Pgp tryptic fragments, the mouse anti-Pgp monoclonal antibodies C219 (Centocor Corp., Philadelphia, PA) and MD7 and MD13 (*37*) (generous gifts of Dr. Victor Ling, Vancouver) were used. Blots were blocked overnight at 4 °C in a solution containing 1% bovine serum albumin (fraction V, fatty acid free) in TBST (10 mM Tris, pH 8.0, 150 mM NaCl, 0.05% Tween-20). This was followed by incubation for 1 h at room temperature with anti-Pgp antibodies used at 1 μg/mL. Specific immune complexes were detected using a second goat anti-mouse antibody (1:10 000 dilution) coupled to peroxidase, and revealed by enhanced chemiluminescence (NEN). When different antibodies were used for the same nitrocellulose membrane, the membranes were stripped as described in the ECL detection system protocol before immunodetection with another antibody. Briefly, the membranes were submerged in stripping buffer (100 mM β-mercaptoethanol, 2% SDS, 62.5 mM Tris-HCl, pH 6.8) and incubated at 50 °C for 30 min with occasional agitation. The membranes were next washed 5 × 10 min in TBST at room temperature using large volumes of TBST followed by a blocking overnight at 4 °C in a solution containing 1% bovine serum albumin (fraction V, fatty acid free) in TBST. Every condition was repeated at least 3 times.

Routine Procedures. Protein concentrations were determined by the bicinchoninic acid method (Pierce) in the presence of 1% SDS using bovine serum albumin as a standard. SDS−PAGE was performed according to Laemmli (*38*) using the Mini-PROTEAN II gel and Electrotransfer system (BioRad).

Materials. Acetone/ether-precipitated *E. coli* lipids were from Avanti Polar Lipids. *n*-Dodecyl-β-D-maltoside was purchased from Anatrace. General chemicals including trypsin (EC 3.4.21.4) type XIII from bovine pancreas were of reagent grade and were purchased from Sigma.

RESULTS

Sensitivity of Pgp to Trypsin in the Presence of Different Nucleotides. In certain proteins, interaction with substrates for catalytic activity induces conformational changes that can be detected by alterations in accessibility of proteolytic cleavage sites. This approach has been used previously to visualize by immunoblotting two Pgp conformations induced by incubation with nucleotides and/or drugs in membrane vesicles (*35*, *36*). It was also demonstrated that $MgCl_2$ alone, $MgCl_2$ with the various nucleotides, and vanadate at concentrations used here have little if any effect on trypsin activity (*35*). In the present study, we have used mouse Mdr3 Pgp which has been purified to homogeneity from overexpressing yeast *P. pastoris* cells, followed by reconstitution in lipids. Such Pgp preparations demonstrate robust ATPase activity stimulated by Pgp substrates and inhibitors (V_{max} = 4.2 μmol min^{-1} mg^{-1}; K_M = 0.7 mM) (*15*). The goal of the present study was to monitor in this purified Pgp preparation conformational changes induced by incubation with hydrolyzable and nonhydrolyzable nucleotides. In addition, we wished to test the effect of discrete mutations introduced in either or both of the NBDs of Pgp on possible nucleotide-induced conformational changes detected in the wild-type protein. Thus, reconstitued Pgp was incubated (15 min) with either $MgCl_2$ alone, MgAMP·PNP, MgADP, MgATP, or MgATP + vanadate (to induce nucleotide trapping) followed by limited trypsin digestion (15 min) with increasing amounts of trypsin. These experiments were done at 37 °C to allow nucleotide binding, ATP hydrolysis, and full trypsin activity, and the Mg^{2+}-nucleotide (10 mM) and vanadate (200 μM) concentrations were those used to demonstrate full ATPase activity of Mdr3 (*15*). The reactions were stopped, and tryptic digestion fragments were separated by SDS−PAGE (12% acrylamide), followed by immunoblotting with the monoclonal anti-Pgp antibody C219. C219 recognizes the epitope VVQ(E/A)ALD (positions 564−570 and 1209−1215) in the large intracellular loops containing each NBD (*39*), and separated by a trypsin-hypersensitive site present in the linker domain of the protein (*40*, *41*) (Figure 1). Therefore, this approach allows one to analyze immunoreactive partial and complete trypsin digestion products derived from both NBDs of the protein. It may be noted that in some of the blots the total immunoreactive signal in the tryptic fragments was far greater than the initial signal detected with the full-length protein. This could be due to differences in better transfer and retention of small fragments compared to the full-length protein or due to increased accessibility of the antibody for its epitope in the smaller denaturated fragments, or both.

The C219-immunoreactive digestion products of reconstitued Pgp observed under control, nucleotide-free conditions ($MgCl_2$ alone) are shown in Figure 2A. Several partial digestion products are generated from the full-length protein, including four fairly stable intermediates labeled W, X, Y, and Z and of molecular mass 66, 60, 44, and 41 kDa, respectively. An additional partial cleavage product of molecular mass around 72 kDa is also detected at low trypsin concentration (see band P in Figure 5). This product is caused by initial cleavage of Pgp at heterogeneous sites within the linker region separating the two halves of the protein (see Discussion). Peptides Y and Z appear at higher trypsin-to-protein ratios than peptides W and X, and must therefore be digestion products of the latter. We monitored the effect of different nucleotide conditions on the appearance and proteolytic resistance of these four tryptic fragments (Figure 2B−D). The observed differences in trypsin cleavage patterns were highly reproducible. In general, we noted that incubation of Pgp with hydrolyzable and nonhydrolyzable nucleotides resulted in trypsin digestion profiles suggestive of increased resistance to protease cleavage. MgAMP·PNP is the nonhydrolyzable analogue of MgATP that competes for MgATP binding to Pgp (*42*, *43*). In the presence of MgAMP·

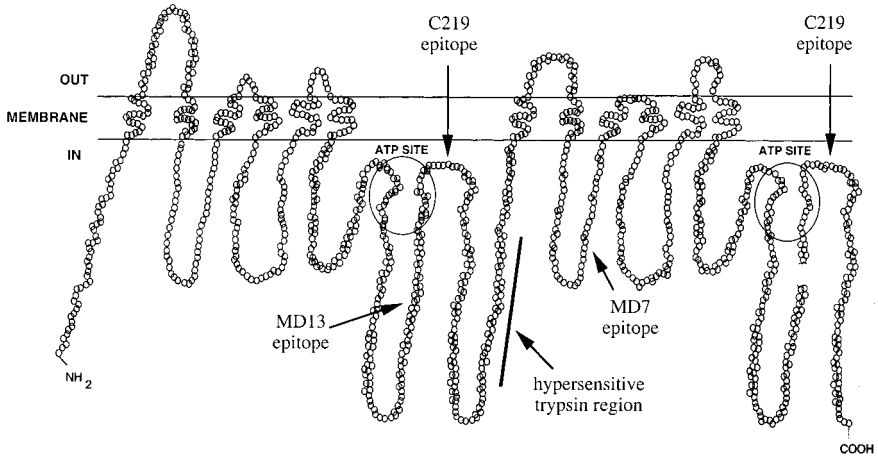

FIGURE 1: Topology of Pgp and localization of the C219, MD7, and MD13 epitopes, the hypersensitive trypsin site, and the nucleotide binding sites (modified from ref *64*).

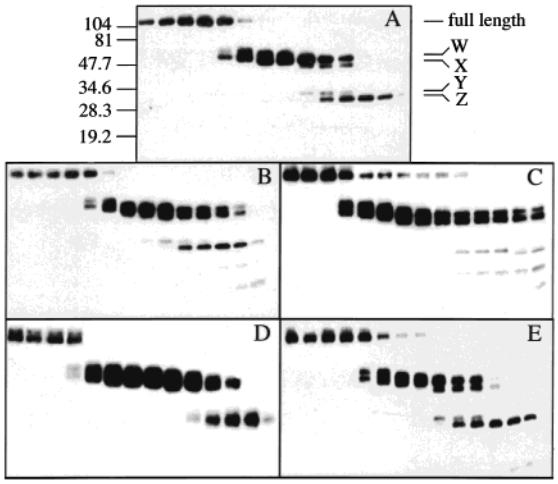

FIGURE 2: Trypsin digestion profiles of wild-type Mdr3 in the presence of 10 mM $MgCl_2$ alone (A), 10 mM MgAMP·PNP (B), 10 mM MgATP + 200 μM vanadate (C), 10 mM MgADP (D), or 10 mM MgATP (E). Purified dialyzed proteins were incubated 15 min at 37 °C in the presence of the indicated substrate, followed by digestion with trypsin, at different trypsin:protein ratios, at 37 °C for 15 min. The reactions were stopped by addition of sample buffer. The peptide fragments were separated on a 12% SDS−PAGE and transferred on a nitrocellulose membrane. Pgp and its fragments were detected by the mouse monoclonal antibody C219.

PNP (Figure 2B), initial cleavage of full-length Pgp was seen at the same trypsin:protein ratio as that required to cleave Pgp in control $MgCl_2$ condition. However, incubation with MgAMP·PNP increased the stability of fragments X and W considerably. These results suggested that the binding of MgAMP·PNP to Pgp induced a more compact conformation than the nucleotide-free one. As MgAMP·PNP is a nonhydrolyzable ATP analogue, the pattern detected may correspond to a stabilized nucleotide triphosphate-bound conformation of Pgp. Incubation of Pgp with MgADP (Figure 2D) also increased the stability of peptides W and Z, while peptides X and Y were difficult to detect. As MgADP is a very poor substrate for Pgp (*43*), this conformation may correspond to a stabilized MgADP-bound form of the protein. Likewise, incubation of Pgp with MgATP prior to trypsin digestion also increased the trypsin resistance of peptides Y and Z, while the sensitivity of the full-length protein was similar to that seen in $MgCl_2$ alone or with MgAMP·PNP incubation conditions (Figure 2E). Since the Pgp used here is active and capable of hydrolyzing MgATP, it is likely that the trypsin digestion profile detected under this condition corresponds to a combination of different conformations (unbound, MgAMP·PNP, or MgADP-bound).

Vanadate induces trapping of nucleotides in the catalytic sites of Pgp, resulting in the generation of a stably inhibited enzyme species. Moreover, the stable vanadate−nucleotide−enzyme complex is thought to resemble the catalytic transition state of the protein (*44*, *45*). Results in Figure 2C indicate that this nucleotide-trapped condition (MgATP + vanadate) induced the most dramatic change in trypsin sensitivity of the wild-type protein. This unique conformation was characterized by a small increase in sensitivity of the full-length protein to initial cleavage by trypsin, but also by a dramatic increased resistance of peptides W and X to trypsin cleavage (when compared to all other conditions). Further digestion of peptides W and X into peptides Y and Z was almost completely inhibited under these conditions (Figure 2C). The effect of MgATP and vanadate on Pgp trypsin sensitivity was specific and not the result of an indirect effect on trypsin activity since this conformation was not detected in vanadate alone (data not shown) or with MgATP alone (Figure 2E). These results indicate that vanadate-induced trapping of nucleotide in Pgp seems to induce a unique conformational change in the stabilized and inhibited enzyme that shows enhanced resistance to trypsin.

Trypsin Sensitivity of Pgp Mutants Bearing Mutations in both Nucleotide Binding Domains. To determine if the unique MgATP + vanadate-induced conformational state of Pgp detected by trypsin sensitivity (Figure 2C) is specific, and possibly corresponds to a catalytic intermediate of the protein, we monitored the appearance of this conformation in catalytically inactive Pgp mutants. We previously reported on the expression, purification, and biochemical characterization of Pgp mutants bearing mutations in both nucleotide binding domains of Pgp, either at the key lysine of the Walker A motif (K429R/K1072R) or at the key aspartate of the Walker B motif (D551N/D1196N). Although these mutations do not impair ATP binding to the protein, they abrogate ATPase activity as measured by a P_i release assay and by the inability to detect vanadate-induced trapping of 8-azido[α-^{32}P]ADP (*15*, *16*). Thus, the K429R/K1072R and D551N/D1196N Pgp mutants were purified to homogeneity and reconstituted in lipids, and their sensitivity to limited

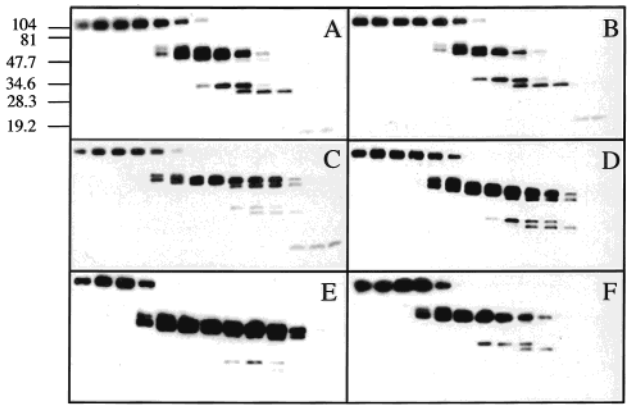

FIGURE 3: Trypsin digestion profiles of Mdr3 double mutants in Walker A (K429R, K1072R) and Walker B (D551N, D1196N) motifs in the presence of 10 mM $MgCl_2$ alone (A and B, respectively), 10 mM MgATP (C and D, respectively), or 10 mM MgATP + 200 μM vanadate (E and F, respectively). Incubation with nucleotides, trypsin digestion, electrophoresis, transfer, and immunodetection with C219 were carried out as described in Figure 2.

trypsin digestion was analyzed in the presence of $MgCl_2$ alone, MgATP, and MgATP + vanadate and compared to that observed for the wild-type protein. The described differences in trypsin cleavage patterns for these mutants were highly reproducible.

In the nucleotide-free $MgCl_2$ control condition (Figure 3A/B), the trypsin digestion profiles of K429R/K1072R (Figure 3A) and D551N/D1196N (Figure 3B) were indistinguishable. The pattern was similar to that of wild-type Pgp (Figure 2A); however, both mutants showed somewhat increased trypsin sensitivity, with fragment X difficult to detect, and fragments W, Y, and Z more sensitive to trypsin cleavage than in the wild-type counterpart (Figure 2A). These results suggested that mutation at Walker A or B motifs in both NBDs may have a small structural effect on the nucleotide-free conformation of Pgp. Both mutants also showed very similar tryptic digestion profiles upon incubation with MgATP (Figure 3C/D). This common pattern was also fairly similar to that seen in wild-type protein except for increased sensitivity of peptide Z compared to wild-type Pgp. However different results were obtained when mutants were analyzed for trypsin sensitivity in the presence of MgATP + vanadate (Figure 3E/F). Indeed, both mutants displayed a fairly similar profile of tryptic fragments, varying only by the sensitivity of the W and X peptides, which were more resistant in the Walker A mutant (K429R/K1072R; Figure 3E) compared to the Walker B mutant (D551N/D1196N; Figure 3F). However, the tryptic digestion profiles of both mutants were strikingly different from that detected in the wild-type protein (Figure 2C). In particular, the high degree of resistance noted for fragments W and X in the wild-type protein (Figure 2C) was not seen in both double mutants. These results indicate that the two double mutants, K429R/K1072R and D551N/D1196N, analyzed cannot adopt the (MgATP + vanadate)-induced conformation detected in the wild-type Pgp. Since these two mutants are catalytically inactive, and cannot trap 8-azido-[α-^{32}P]ADP in the presence of vanadate (*15*), our results suggest that the unique (MgATP + vanadate)-induced conformation seen in wild-type Pgp may correspond to the nucleotide-trapped catalytic intermediate of Pgp.

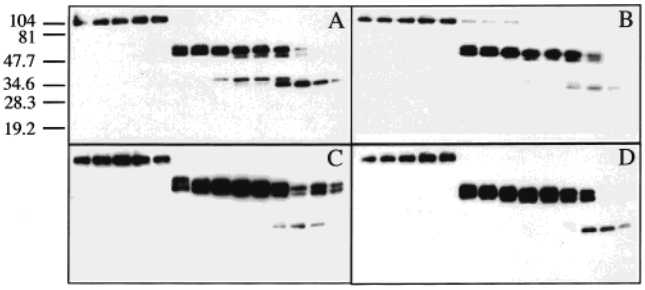

FIGURE 4: Trypsin digestion profiles of Mdr3 single mutant K429R (A), K1072R (B), D551N (C), and D1196N (D) in the presence of 10 mM MgATP + 200 μM vanadate. Incubation with nucleotide, trypsin digestion, electrophoresis, transfer, and immunodetection with C219 were carried out as described in Figure 2.

Trypsin Sensitivity of Pgp Mutants Bearing Single Mutations in either Nucleotide Binding Domain. Although it has been clearly established that both NBDs of Pgp are absolutely required for function, there has been some debate in the literature concerning the structural and functional equivalence of these two NBDs in the alternate site catalysis model for ATP hydrolysis proposed by Senior et al. (*46*) (see Discussion). Thus, we purified Pgp mutants bearing single amino acid substitutions in either NBD1 (K429R, D551N) or NBD2 (K1072R, D1196N) and analyzed their trypsin digestion profiles in the presence of MgATP + vanadate (Figure 4). We have previously shown that these mutants cannot confer drug resistance in transfection assay (*13*) and have no detectable ATPase activity (*15*). Under nucleotide-free conditions ($MgCl_2$ alone), all four mutants showed similar digestion profiles (data not shown). When analyzed in the presence of MgATP and vanadate, several observations were made. First, all four mutants showed very similar sensitivity of initial cleavage of the full-length protein (Figure 4A−D). Second, trypsin sensitivity of the diagnostic fragments W and X was very similar for the mutants K429R (Figure 4A), K1072R (Figure 4B), and D1196N (Figure 4D), but, in contrast to wild-type Pgp, these fragments were absent at the highest trypsin:Pgp ratios. Third, the D551N Walker B mutant in NBD1 (Figure 4C) had a trypsin digestion profile that was different from the other three mutants analyzed, and that resembled that seen for wild-type Pgp (Figure 2C). Indeed, fragments W and X were still detected in this mutant even at the highest trypsin:Pgp ratio (Figure 4C). Similar results were obtained in three independent experiments using two independent preparations of the mutant proteins. The surprising similarity between the trypsin digestion profiles of D551N (Figure 4C) and wild-type Pgp (Figure 2C) under MgATP + vanadate conditions suggests that D551N can adopt a conformation related to that seen in the wild-type protein under conditions of vanadate-induced trapping of nucleotide.

Identification of Trypsin Digestion Products of Wild-Type and Mutant Pgps. The nature and possible location in the mature protein of tryptic Pgp peptides generated under conditions of MgATP + vanadate were investigated by epitope mapping. Immunoblots of tryptic digests from wild-type Pgp, D551N, as well as D1196N and K429R, that show different conformations under vanadate-induced trapping conditions, were analyzed using two additional monoclonal anti-Pgp antibodies, MD7 and MD13 (Figure 1). C219 (Figures 5A, 6A, 7A, and 8A) recognizes two epitopes within

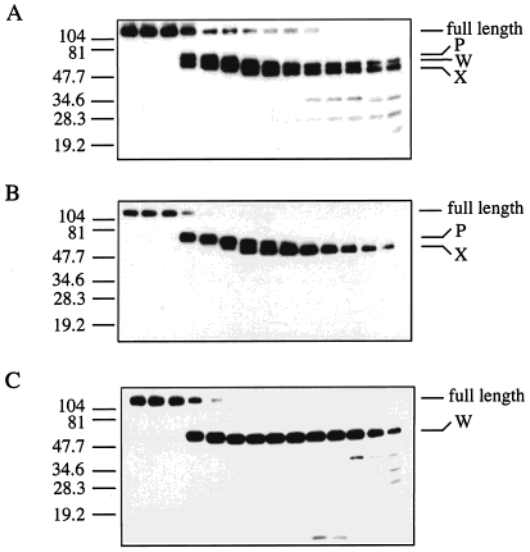

FIGURE 5: Trypsin digestion profiles of wild-type Mdr3 in the presence of 10 mM MgATP + 200 μM vanadate. Incubation with nucleotide, trypsin digestion, electrophoresis, and transfer were carried out as described in Figure 2. Membrane from Figure 2C was stripped before immunodetection with two different mouse anti-Pgp monoclonal antibodies: MD7 (B) and MD13 (C). Immunodetection with the mouse monoclonal antibody C219 (A) was shown as a control (identical to Figure 2C). C219 recognizes two epitopes within each half of Pgp. MD7 recognizes a short peptide at positions 804−814, within the predicted intracellular loop separating predicted TM domains 8 and 9, and is specific for the C-terminal half of Pgp. MD13 recognizes a peptide sequence (positions 494−504) in the N-terminal half of Pgp within the NBD1, and does not appear to cross-react with the homologous segment of the C-terminal half of Pgp. After each immunodetection, the membranes were stripped as described under Experimental Procedures before immunodetection with another antibody.

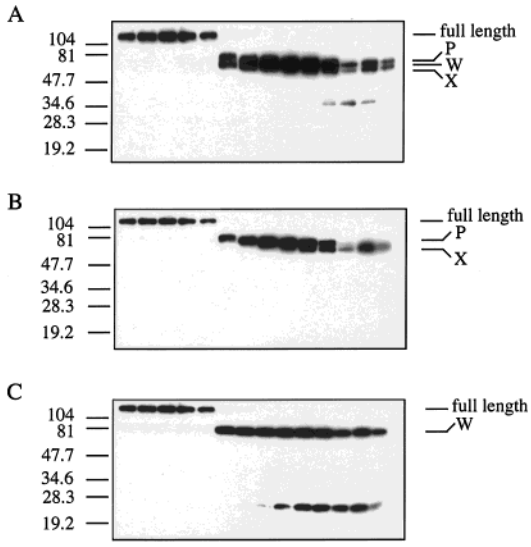

FIGURE 6: Trypsin digestion profiles of Mdr3 single mutant D551N in the presence of 10 mM MgATP + 200 μM vanadate. Membrane from Figure 4C was stripped before immunodetection with two different mouse anti-Pgp monoclonal antibodies: MD7 (B) and MD13 (C). Immunodetection with mouse monoclonal antibody C219 (A) was shown as a control (identical to Figure 4C). Incubation with nucleotide, trypsin digestion, electrophoresis, transfer, and stripping were carried out as described in Figure 5.

each half of Pgp (*39*). MD7 (Figures 5B, 6B, 7B, and 8B) recognizes a short peptide at positions 804−814, within the predicted intracellular loop separating predicting TM domains

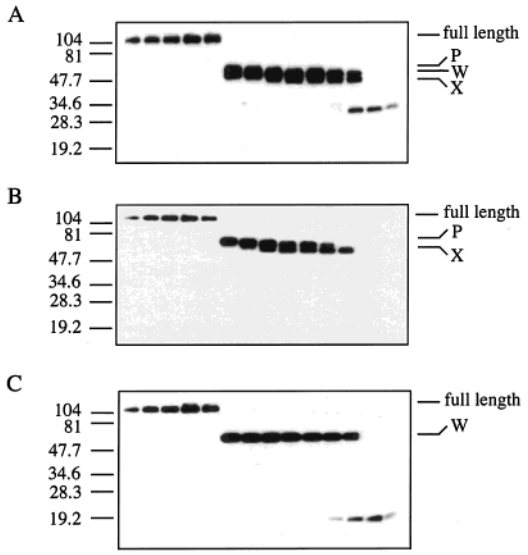

FIGURE 7: Trypsin digestion profiles of Mdr3 single mutant D1196N (D) in the presence of 10 mM MgATP + 200 μM vanadate. Membrane from Figure 4D was stripped before immunodetection with two different mouse anti-Pgp monoclonal antibodies: MD7 (B) and MD13 (C). Immunodetection with the mouse monoclonal antibody C219 (A) was shown as a control (identical to Figure 4D). Incubation with nucleotide, trypsin digestion, electrophoresis, transfer, and stripping were carried out as described in Figure 5.

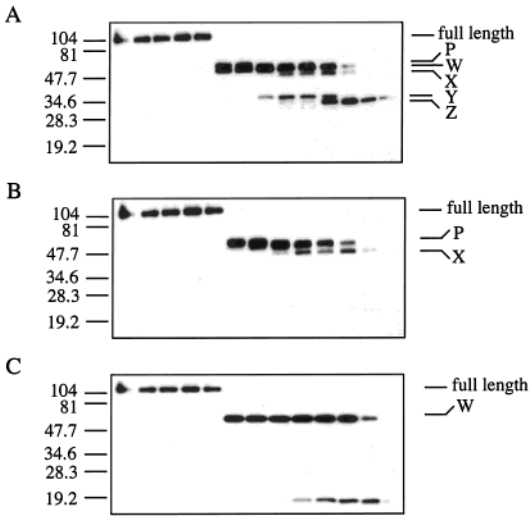

FIGURE 8: Trypsin digestion profiles of Mdr3 single mutant K429R in the presence of 10 mM MgATP + 200 μM vanadate. Membrane from Figure 4A was stripped before immunodetection with two different mouse anti-Pgp monoclonal antibodies: MD7 (B) and MD13 (C). Immunodetection with mouse monoclonal antibody C219 (A) was shown as a control (identical to Figure 4A). Incubation with nucleotide, trypsin digestion, electrophoresis, transfer, and stripping were carried out as described in Figure 5.

8 and 9, and is specific for the C-terminal half of Pgp (*37*). MD13 (Figures 5C, 6C, 7C, and 8C) recognizes a peptide sequence (positions 494−504) in the N-terminal half of Pgp within the NBD1 (*37*), and does not appear to cross-react with the homologous segment of the C-terminal half of Pgp (see below). Trypsin treatment of the full-length wild-type Pgp or D551N mutant generates three major C219-reactive fragments that are labeled P, W, and X in Figures 5A and 6A. The first detectable trypsin cleavage generates two products, P and W (at low trypsin doses), probably through

cleavage at the hypersensitive site previously mapped in the linker domain of the protein (*40, 41*). Upon increased trypsin digestion, peptide P appears progressively degraded into peptide X (Figures 5B and 6B). Peptides P and X are recognized specifically by MD13 and are from the N-terminal half of Pgp (Figures 5B and 6B). The progressive degradation of P into X may result from cleavage at multiple sites within the lysine- and arginine-rich linker domain of the protein, located C-terminal of the MD13 epitope (Figure 1). Peptide W is recognized by MD7 (Figures 5C and 6C), shows a distinct appearance profile, is one of the two products of initial trypsin cleavage of the full-length protein, and represents the C-terminal half of Pgp. Under MgATP + vanadate conditions, both peptides W and X were highly resistant to trypsin in wild-type and D551N proteins. We were unable to accurately determine the location of smaller tryptic fragments generated at very high trypsin:Pgp ratios. The K429R (Figure 7) and D1196N (Figure 8) mutants showed a similar tryptic profile for fragments P, W, and X at low trypsin:Pgp ratios. However, they showed greatly enhanced sensitivity to trypsin digestion compared to wild-type Pgp which allowed visualization of the C219-immunoreactive peptides Y and Z. However, peptides Y and Z do not react with either MD7 or MD13 but react with the polyclonal anti-Pgp antibody PEG-12 (data not shown). PEG-12 recognizes a peptide epitope at positions 1083−1178, close to NBD2, and is specific for the C-terminal half of Pgp (*47*). These results indicate that the 44 and 41 kDa peptides Y and Z are derived from the C-terminal domain of Pgp. These results also suggest that Y and Z are generated by cleavage at a site or sites located in the interval separating the MD7 (804−814) and PEG-12 (1083−1178) epitopes in the C-terminal half of Pgp.

Together, the results indicate that in the wild-type and D551N proteins, conditions of vanadate-induced nucleotide trapping induce a conformation that shows increased trypsin resistance of both halves of Pgp, while this is not seen in the K429R and D1196N mutants.

DISCUSSION

In the absence of high-resolution structural information for Pgp, techniques such as hydropathy profiling (*48, 49*), accessibility to protease cleavage sites (*50*), epitope mapping of inserted antigenic peptides (*51*), photoaffinity labeling (*52*), and modification by sulfhydryl reagents (*53*) have been used to identify major secondary structure features of the protein, and to establish structure/function relationships. In addition, differential immunoreactivity (*19*), sensitivity to protease cleavage (*35, 36*), quenching of fluorescently labeled residues (NBD-Cl, MIANS, MANT-ATP) (*29, 54, 55*), and infrared spectroscopy (*25*) have been used to monitor overall conformational changes and changes in the local environment of specific residues caused by interaction of Pgp with lipids, nulceotides, and drug substrates. In particular, Wang et al. (*35*) have used trypsin sensitivity to monitor nucleotide-induced conformational changes in Pgp, using Pgp expressed in membrane vesicles from multidrug resistant cells, and Western blotting with anti-Pgp monoclonal antibody MD7. This antibody recognizes an epitope located in the TM8−TM9 intervening segment of Pgp, and thus allows monitoring of changes in tryptic digestion products derived from the C-terminal half of Pgp. Using this approach, two major Pgp conformations could be detected, one in the presence of MgADP or MgATP, and the other in the presence of $MgCl_2$, MgAMP·PNP, or MgATP with vanadate. These two conformations were distinguished by the presence or absence of a diagnostic MD-7 immunoreactive 19 kDa tryptic Pgp fragment. Additional studies from the same group indicated that incubation of Pgp with vinblastine or verapamil also caused a change in intensity of MD-7 immunoreactive tryptic fragments of 17 and 19 kDa (*36*). Although these studies were somewhat limited by (a) the use of Pgp in membrane vesicles (where all cleavage sites may not be accessible), (b) the use of a single antibody directed against the C-terminal half only, and (c) the use of a single trypsin dose, these experiments nevertheless demonstrate elegantly that conformational changes in Pgp can be monitored by trypsin sensitivity.

In the present study, we have used trypsin sensitivity to monitor conformational changes in Pgp caused by nucleotides under either binding or hydrolysis conditions. These experiments were conducted using highly purified Pgp prepared from overexpressing *P. pastoris* cells (*15*), and reconstituted in *E. coli* lipids. Such preparations have full ATPase activity (V_{max} = 4.2 μmol min^{-1} mg^{-1}, K_M = 0.7 mM), similar to that measured in human and hamster Pgp preparations purified from mammalian cells (*3, 11, 43*). For protease sensitivity, we used a wide range of 14 trypsin concentrations that facilitate semiquantitative evaluation of sensitivity to cleavage of individual partial digestion products. Partial tryptic digestion products were revealed by immunoblotting, using the mouse monoclonal anti-Pgp antibody C219, which recognizes an epitope in both NB sites of the protein and thus allows monitoring of changes in trypsin sensitivity in both halves of the protein. In addition, we have investigated the effect of mutations in either or both Pgp NBDs on these nucleotide-induced conformational changes. The loss-of-function phenotype of these mutants had been previously characterized biochemically in the same Pgp preparations purified from *P. pastoris* (*15*). In the experimental conditions used, studies with antibodies directed against each half of Pgp (Figures 5−8) showed that in increasing trypsin doses, Pgp is initially cleaved in the linker region to produce two large fragments (P and W). This observation is in agreement with previous data mapping a protease hypersensitive site in the Pgp linker domain (*40, 41*). The P fragment corresponding to the N-terminal half is progressively digested into fragment X, possibly by additional cleavage within the linker region. At higher trypsin doses, W and X are further cleaved into two smaller fragments (Y and Z) possibly corresponding to the C-terminal half of Pgp. The intensity of these tryptic fragments was monitored under different nucleotide conditions, and compared to that of control nucleotide-free $MgCl_2$ conditions. Although several related conformations could be tentatively identified, the most dramatic and obvious change was that seen upon incubation with MgATP + vanadate (nucleotide-trapped condition). Vanadate-induced trapping induced a conformation highly resistant to trypsin cleavage (when compared to $MgCl_2$, MgADP, MgATP conditions), including persistence of fragments W and X, and absence of fragments Y and Z, even at the highest trypsin dose tested (Figure 2C). Orthovanadate is a potent inhibitor of Pgp ATPase. Vanadate is a transition state analogue that blocks Pgp in the MgADP-bound form, resulting in the production

of a stable Pgp·MgADP·Vi complex after hydrolysis of the γ-phosphate of MgATP by wild-type, catalytically active Pgp (*44, 56*). Our observations that this conformation is not seen when wild-type Pgp is incubated with vanadate alone (data not shown) or with MgATP (Figure 2E), and is abolished in the catalytically inactive K429R/K1072R and D551N/D1196N double mutants (Figures 3E/F), together suggest that this conformation indeed corresponds to a nucleotide-bound and catalytically inhibited form of the protein. It is interesting to note that, based on susceptibility to trypsin cleavage (persistance of fragments W and X), the conformation most closely related to the nucleotide-trapped one is that seen for the nonhydrolyzable AMP·PNP nucleotide (Figure 2B). Wang et al. (*35*) compared conformational changes induced by MgATP and MgATP + vanadate in Pgp expressed in membrane vesicles. Although the diagnostic Pgp fragments seen in the MgATP form were absent in the MgATP + vanadate form, they could not determine the uniqueness of the latter conformation as its pattern of MD-7 reactive peptides was similar to that seen in the absence of nucleotides ($MgCl_2$ alone).

Pgp has been proposed to hydrolyze ATP by an alternate site catalysis model, where both sites bind and hydrolyze ATP in an alternate fashion, and with complete cooperativity between the two sites (*11, 46*). This is supported by the observations that (1) mutations in or chemical modifications of either of the two sites completely inactivate ATP hydrolysis and drug transport by the protein (*13, 15, 17*); (2) in photolabeling experiments, the strong inhibitor of Pgp ATPase vanadate seems to induce trapping of a single nucleotide per Pgp molecule (MgADP), that can be cross-linked at either NB site (*44, 45*), indicating that hydrolysis and trapping at one site prevent hydrolysis at the other site. The functional equivalence of the two NBDs in this process is still not fully understood, and possible differences between the two sites have been documented (*16*, see discussion below). Thus, the nucleotide-bound/inhibited conformation of wild-type Pgp detected with trypsin (Figure 2C) was examined in a number of Pgp mutants bearing single or double inactivating mutations at key residues of the Walker A (K429R, K1072R) and Walker B (D551N, D1196N) motifs of the predicted NBDs. Previous studies from our group have shown that these mutants can bind but cannot hydrolyze MgATP, as determined by photolabeling of purified protein with [^{32}P]-8-azido-ATP under binding or trapping conditions, as well as by direct ATP hydrolysis assays (P_i release) (*15*). Although both the double (Figure 3A/B) and single site mutants (data not shown) showed patterns of trypsin sensitivity in nucleotide-free conditions that were similar to each other and similar to wild-type (Figure 2A), important differences were seen under conditions of vanadate-induced trapping. Indeed, the double mutants K429R/K1072R and D551N/D1196N, as well as the single Walker A mutants K429R and K1072R, did not show the vanadate-trapped conformation, in agreement with the biochemical loss of function documented for these mutants (*13, 15*). Unexpectedly, the single Walker B mutants showed different results, with the D1196N mutant showing trypsin sensitivity similar to that of the other inactive mutants while D551N showed a conformation similar to that seen for wild-type Pgp. Thus, mutations at the homologous key aspartate residue of the two NB sites of Pgp induce different conformations under vanadate-induced trapping of nucleotides. This differential effect appears specific as (1) it is not seen for the Walker A lysine mutants, and (2) D551N and D1196N show similar trypsin sensitivity under nucleotide-free conditions (not shown). Although the molecular basis of the distinct behavior of D551N and D1196N remains unclear, this result clearly suggests structural and/or functional differences between the two mutants and hence between the two NBDs of Pgp.

As mentioned previously, several experiments suggest that both NBDs of Pgp are functionally equivalent in the proposed alternate site catalysis mechanism. The two halves of Pgp expressed independently can bind to and hydrolyze ATP with a similar basal ATPase activity (*57*). Mutations in either NBD of Pgp completely abolish drug transport in mammalian cells (*13, 14*). 8-Azido[α-^{32}P]ATP photolabeling and vanadate-induced trapping can occur in each NBD with a cooperative but equivalent role of the two sites (*44, 45, 56, 58*). Mutation in Walker A or B motifs completely abolished ATPase activity with no vanadate-induced trapping of Mg-8-azido-[α-^{32}P]ADP detected for these mutants (*15*). Chemical modification of a single cysteine introduced in either NBD of Pgp results in complete and similar *N*-ethylmaleimide-induced loss of ATPase activity in the protein (*53*).

On the other hand, additional studies of Pgp and other ABC transporters suggest that the two NBDs may not be completely equivalent. Indeed, Hrycyna et al. (*16*) have obtained evidence suggesting functional differences between the two NBDs of human MDR1. In particular, they show that in the wild-type protein photolabeling with [^{32}P]-8-azido-ATP at subsaturating concentrations followed by partial trypsin cleavage and immunoprecipitation shows stronger labeling in the N-terminal NBD (NBD1) than in the C-terminal NBD2. Additional photolabeling experiments using the Walker B mutants D555N and D1200N showed that in contrast to results from Urbatsch et al. (*15*), only the D1200N mutant can be photolabeled under binding conditions with all the label being present at the NBD1 (*16*). By contrast, when vanadate was included in the assay (nucleotide-trapped conditions), the NBD2 of the wild-type protein was preferentially labeled when compared to its NBD1 counterpart, with mutations at both sites abrogating labeling. Similar experiments in another, although distant member of the ABC family CFTR also showed nonsymmetrical labeling of the two NBDs of the protein with [^{32}P]-8-azido ATP. In these studies, the NBD1 of CFTR was preferentially labeled by [^{32}P]-8-azido ATP under binding conditions, while labeling at both sites was detected when vanadate was included in the labeling reaction for trapping (*59*). These results are paralleled by the distinct transport properties of CFTR mutants bearing mutations at homologous residues of each NBD (*60*−*62*). Finally, mutations at the homologous positions in the Walker A and B motifs of other distantly related ABC transporters such as the yeast *S. cerevisiae* **a** factor transporter STE6 (*63*) and the nematode *C. elegans* cell engulfment protein ced-7 (*64*) do not have the same deleterious effect on the overall transport properties of these proteins.

These results are in agreement with those obtained in the current study which show that mutations at equivalent residue in the two halves of Pgp do not have the same effect on the protein conformation under nucleotide trapping conditions.

The current studies strongly suggest possible structural or functional differences between the two NBDs of Pgp.

ACKNOWLEDGMENT

We are indebted to Dr. Victor Ling (British Columbia Cancer Research Center) for the generous gift of the mouse anti-Pgp monoclonal antibodies MD7 and MD13, Dr. Michael Gottesman (NIH, Bethesda, MD) for the generous gift of the rabbit anti-Pgp polyclonal antibody PEG-12, and Dr. Ina Urbatsch for helpful discussion.

REFERENCES

1. Shustik, C., Dalton, W., and Gros, P. (1995) *Mol. Aspects Med. 16*, 1−78.
2. Scarborough, G. A. (1995) *J. Bioenerg. Biomembr. 27*, 37−41.
3. Shapiro, A. B., and Ling, V. (1995) *J. Bioenerg. Biomembr. 27*, 7−13.
4. Dean, M., and Allikmets, R. (1995) *Curr. Opin. Genet. Dev. 5*, 779−785.
5. Harding, C. V., and Geuze, H. J. (1993) *Curr. Opin. Cell Biol. 5*, 596−605.
6. Rich, D. P., Anderson, M. P., Gregory, R. J., Cheng, S. H., Paul, S., Jefferson, D. M., McCann, J. D., Klinger, K. W., Smith, A. E., and Welsh, M. J. (1990) *Nature 347*, 358−363.
7. Kamijo, K., Taketani, S., Yokota, S., Osumi, T., and Hashimoto, T. (1990) *J. Biol. Chem. 265*, 4534−4540.
8. Mosser, J., Douar, A. M., Sarde, C. O., Kioschis, P., Feil, R., Moser, H., Poustka, A. M., Mandel, J. L., and Aubourg, P. (1993) *Nature 361*, 726−730.
9. Gerloff, T., Stieger, B., Hagenbuch, B., Madon, J., Landmann, L., Roth, J., Hofmann, A. F., and Meier, P. J. (1998) *J. Biol. Chem. 273*, 10046−10050.
10. Babenko, A. P., Aguilar-Bryan, L., and Bryan, J. (1998) *Annu. Rev. Physiol. 60*, 667−687.
11. Senior, A. E., Al-Shawi, M. K., and Urbatsch, I. L. (1995b) *J. Bioenerg. Biomembr. 27*, 31−36.
12. Walker, J. E., Saraste, M., Runswick, M. J., and Gay, N. J. (1982) *EMBO J. 1*, 945−951.
13. Azzaria, M., Schurr, E., and Gros, P. (1989) *Mol. Cell. Biol. 9*, 5289−5297.
14. Roninson, I. B. (1992) *Biochem. Pharmacol. 43*, 95−102.
15. Urbatsch, I. L., Beaudet, L., Carrier, I., and Gros, P. (1998) *Biochemistry 37*, 4592−4602.
16. Hrycyna, C. A., Ramachandra, M., Germann, U. A., Cheng, P. W., Pastan, I., and Gottesman, M. M. (1999) *Biochemistry 38*, 13887−13899.
17. Loo, T. P., and Clarke, D. M. (1995a) *J. Biol. Chem. 270*, 21449−21452.
18. Senior, A. E., and Gadsby, D. C. (1997) *Semin. Cancer Biol. 8*, 143−150.
19. Mechetner, E. B., Schott, B., Morse, B. S., Stein, W. D., Druley, T., Davis, K. A., Tsuruo, T., and Roninson, I. B. (1997) *Proc. Natl. Acad. Sci. U.S.A. 94*, 12908−12913.
20. Weber, J., Wilke-Mounts, S., Lee, R. S.-F., Grell, E., and Senior, A. E. (1993) *J. Biol. Chem. 268*, 20126−20133.
21. Weber, J., and Senior, A. E. (1997) *Biochim. Biophys. Acta 1319*, 19−58.
22. Zhou, T., and Rosen, B. P. (1997) *J. Biol. Chem. 272*, 19731−19737.
23. Walmsley, A. R., Zhou, T., Borges-Walmsley, M. I., and Rosen, B. P. (1999) *J. Biol. Chem. 274*, 16153−16161.
24. Menezes, M. A., Roepe, P. D., and Kaback, H. R. (1990) *Proc. Natl. Acad. Sci. U.S.A. 87*, 1638−1642.
25. Sonveaux, N., Shapiro, A. B., Goormaghtigh, E., Ling, V., and Ruysschaert, J. M. (1996) *J. Biol. Chem. 271*, 24617−24624.
26. Sonveaux, N., Vigano, C., Shapiro, A. B., Ling, V., and Ruysschaert, J.-M. (1999) *J. Biol. Chem. 274*, 17649−17654.
27. Liu, R., and Sharom, F. J. (1996) *Biochemistry 35*, 11865−11873.
28. Liu, R., and Sharom, F. J. (1997) *Biochemistry 36*, 2836−2843.
29. Liu, R., and Sharom, F. J. (1998) *Biochemistry 37*, 6503−6512.
30. Gomes, X. V., Henricksen, L. A., and Wold, M. S. (1996) *Biochemistry 35*, 5586−5595.
31. Stout, J. G., Zhou, Q., Wiedmer, T., and Sims, P. J. (1998) *Biochemistry 37*, 14860−14866.
32. Rothman, A., Gerchman, Y., Padan, E., and Schuldiner, S. (1997) *Biochemistry 36*, 14572−14576.
33. Morsomme, P., Dambly, S., Maudoux, O., and Boutry, M. (1998) *J. Biol. Chem. 273*, 34837−34842.
34. Zhang, F., Kartner, N., and Lukacs, G. L. (1998) *Nat. Struct. Biol. 5*, 180−183.
35. Wang, G., Pincheira, R., Zhang, M., and Zhang, J.-T. (1997) *Biochem. J. 328*, 897−904.
36. Wang, G., Pincheira, R., and Zhang, J.-T. (1998) *Eur. J. Biochem. 255*, 383−390.
37. Shapiro, A., Duthie, M., Childs, S., Okubo, T., and Ling, V. (1996) *Int. J. Cancer 67*, 256−263.
38. Laemmli, U. K. (1970) *Nature 227*, 680−683.
39. Georges, E., Bradley, G., Gariepy, J., and Ling, V. (1990) *Proc. Natl. Acad. Sci. U.S.A. 87*, 152−156.
40. Bruggemann, E. P., Germann, U. A., Gottesman, M. M., and Pastan, I. (1989) *J. Biol. Chem. 264*, 15483−15488.
41. Georges, E., Zhang, J.-T., and Ling, V. (1991) *J. Cell. Physiol. 148*, 479−484.
42. Al-Shawi, M. K., Urbatsch, I. L., and Senior, A. E. (1994) *J. Biol. Chem. 269*, 8986−8992.
43. Urbatsch, I. L., Al-Shawi, M. K., and Senior, A. E. (1994) *Biochemistry 33*, 7069−7076.
44. Urbatsch, I., Sankaran, B., Weber, J., and Senior, A. E. (1995a) *J. Biol. Chem. 270*, 19383−19390.
45. Hrycyna, C. A., Ramachandra, M., Ambudkar, S. V., Ko, Y. H., Pedersen, P. L., Pastan, I., and Gottesman, M. M. (1998) *J. Biol. Chem. 273*, 16631−16634.
46. Senior, A. E., Al-Shawi, M. K., and Urbatsch, I. L. (1995a) *FEBS Lett. 377*, 285−289.
47. Bruggemann, E. P., Chaudhary, V., Gottesman, M. M., and Pastan, I. (1991) *BioTechniques 10*, 202−209.
48. Gros, P., Croop, J., and Housman, P. (1986) *Cell 47*, 371−380.
49. Chen, C. J., Chin, J. E., Ueda, K., Clark, K., Clark, D. P., Pastan, I., Gottesman, M. M., and Roninson, I. B. (1986) *Cell 47*, 381−389.
50. Yoshimura, A., Kuwazura, Y., Sumizawa, T., Ichikawa, M., Ikeda, S., Uda, T., and Akiyama, S. (1989) *J. Biol. Chem. 264*, 16282−16291.
51. Kast C., Canfield, V., Levenson, R., and Gros, P. (1996) *J. Biol. Chem. 271*, 9240−9248.
52. Greenberger, L. M., Lisanti, C. J., Silva, J. T., and Horwitz, S. B. (1991) *J. Biol. Chem. 266*, 20744−20751.
53. Loo, T. P., and Clarke, D. M. (1995b) *J. Biol. Chem. 270*, 22957−22961.
54. Conseil, G., Baubichon-Cortay, H., Dayan, G., Jault, J. M., Barron, D., and Di Pietro, A. (1998) *Proc. Natl. Acad. Sci. U.S.A. 95*, 9831−9836.
55. Romsicki, Y., and Sharom, F. J. (1999) *Biochemistry 38*, 6887−6896.
56. Urbatsch, I., Sankaran, B., Bhagat, S., and Senior, A. E. (1995b) *J. Biol. Chem. 270*, 26956−26961.
57. Loo, T. P., and Clarke, D. M. (1994) *J. Biol. Chem. 269*, 7750−7755.
58. Szabo, K., Welker, E., Bakos, E., Muller, M., Roninson, I. B., Varadi, A., and Sarkadi, B. (1998) *J. Biol. Chem. 273*, 10132−10138.
59. Szabo, K., Szakacs, G., Hegedus, T., and Sarkadi, B. (1999) *J. Biol. Chem. 274*, 12209−12212.

60. Ramjeesingh, M., Li, C., Garami, E., Huan, L.-J., Galley, K., Wang, Y., and Bear, C. E. (1999) *Biochemistry 38*, 1463−1468.
61. Carson, M. R., Travis, S. M., and Welsh, M. J. (1995) *J. Biol. Chem. 270*, 1711−1717.
62. Gadsby, D. C., and Nairn, A. C. (1999) *Physiol. Rev. 79*, S77−S107.
63. Berkower, C., and Michaelis, S. (1991) *EMBO J. 12*, 3777−3785.
64. Wu, Y.-C., and Horvitch, H. R. (1998) *Cell 93*, 951−960.
65. Gottesman, M. M., and Pastan, I. (1988) *J. Biol. Chem. 263*, 12163−12166.

BI992744Z